Radiotherapy and Oncology 166 (2022) 44–50

Contents lists available at ScienceDirect

Radiotherapy and Oncology

journal homepage: www.thegreenjournal.com

Original Article

First demonstration of the FLASH effect with ultrahigh dose rate high-energy X-rays

Feng Gao [a], Yiwei Yang [b,1], Hongyu Zhu [c,1], Jianxin Wang [d], Dexin Xiao [d], Zheng Zhou [d], Tangzhi Dai [a], Yu Zhang [a], Gang Feng [a], Jie Li [a], Binwei Lin [a], Gang Xie [e], Qi Ke [e], Kui Zhou [d], Peng Li [d], Xuming Shen [d], Hanbin Wang [d], Longgang Yan [d], Chenglong Lao [d], Lijun Shan [d], Ming Li [d], Yanhua Lu [d], Menxue Chen [d], Song Feng [f], Jianheng Zhao [d], Dai Wu [d,*], Xiaobo Du [a,*]

[a] Departmant of Oncology, Nuclear Medicine Laboratory of Mianyang Central Hospital, Mianyang Central Hospital, School of Medicine, University of Electronic Science and Technology of China; [b] Institute of Nuclear Physics and Chemistry, China Academy of Engineering Physics, Mianyang; [c] Department of Radiation Oncology, Sun Yat-sen University Cancer Center, State Key Laboratory of Oncology in South China, Collaborative Innovation Center for Cancer Medicine, Guangzhou; [d] Institute of Applied Electronics, China Academy of Engineering Physics; [e] Department of Pathology, Mianyang Central Hospital, School of Medicine, University of Electronic Science and Technology of China, Mianyang; and [f] School of Nuclear Science and Technology, University of South China, Hengyang, China

ARTICLE INFO

Article history:
Received 3 May 2021
Received in revised form 2 October 2021
Accepted 1 November 2021
Available online 11 November 2021

Keywords:
High-energy X-rays
FLASH radiotherapy
Conventional dose rate radiotherapy
FLASH effect

ABSTRACT

Purpose: This study aimed to evaluate whether high-energy X-rays (HEXs) of the PARTER (platform for advanced radiotherapy research) platform built on CTFEL (Chengdu THz Free Electron Laser facility) can produce ultrahigh dose rate (FLASH) X-rays and trigger the FLASH effect.

Materials and methods: EBT3 radiochromic film and fast current transformer (FCT) devices were used to measure absolute dose and pulsed beam current of HEXs. Subcutaneous tumor-bearing mice and healthy mice were treated with sham, FLASH, and conventional dose rate radiotherapy (CONV), respectively to observe the tumor control efficiency and normal tissue damage.

Results: The maximum dose rate of HEXs of PARTER was up to over 1000 Gy/s. Tumor-bearing mice experiment showed a good result on tumor control ($p < 0.0001$) and significant difference in survival curves ($p < 0.005$) among the three groups. In the thorax-irradiated healthy mice experiment, there was a significant difference ($p = 0.038$) in survival among the three groups, with the risk of death decreased by 81% in the FLASH group compared to that in the CONV group. The survival time of healthy mice irradiated in the abdomen in the FLASH group was undoubtedly higher (62.5% of mice were still alive when we stopped observation) than that in the CONV group (7 days).

Conclusion: This study confirmed that HEXs of the PARTER system can produce ultrahigh dose rate X-rays and trigger a FLASH effect, which provides a basis for future scientific research and clinical application of HEX in FLASH radiotherapy.

Cancer is the first or second leading causes of death in humans beings aged less than70 years in 91 of 172 countries, and the third or fourth leading cause of death in another 22 countries [1]. Radiotherapy is one of the most widely used anti-tumor therapy methods [2]; 60–70% of cancer patients need radiotherapy during their cancer treatment process [3].

The conventional dose rate radiotherapy (CONV, ≤0.1 Gy/s) [4] can not only shrink the tumor but also lead to radiation-induced toxicities in normal tissues. Normal tissue complications limit the dose that can be delivered to the tumor. In 2014, the first *in vivo* ultrahigh dose rate (FLASH, >40 Gy/s) radiation experiment was performed and found that tumors can be effectively suppressed while healthy tissues were spared [5]; this phenomenon was termed the FLASH effect. The performance of FLASH was superior to CONV radiotherapy [6]. Therefore, FLASH seemed to be a promising technique for cancer treatment. Although the mechanisms underlying the FLASH effect remain unclear and some negative results have been reported [7], many FLASH studies performed

Abbreviations: HEXs, high-energy X-rays; CTFEL, Chengdu THz Free Electron Laser facility; FCT, fast current transformer; CONV, conventional dose-rate radiotherapy; MC, Monte Carlo.

* Corresponding authors at: Institute of Applied Electronics, China Academy of Engineering Physics, Mianyang 621900, China (D. Wu). Departmant of Oncology, Mianyang Central Hospital, School of Medicine, University of Electronic Science and Technology of China, Mianyang 621000, China (X. Du).

E-mail addresses: wudai04@caep.cn (D. Wu), duxiaobo2005@126.com (X. Du).

[1] Feng Gao , Yiwei Yang and Hongyu Zhu are co-first authors.

https://doi.org/10.1016/j.radonc.2021.11.004
0167-8140/

on animals [5–6,8–14] and the first human treatment in Switzerland showed satisfactory results [15]. Based on the aforementioned studies, the US Food and Drug Administration approved the research device exemption for the first FLASH clinical trial [16].

Electrons [4–5,7,11–13,17–20], kilo-voltage (kVp) X-rays [10,21] and protons [22–24] have been utilized in FLASH preclinical research. Electrons and kVp X-rays are usually used to treat superficial tumor sites but are not suitable for tumors situated deep within the body. Protons can be used to treat deep tumors, but the high construction and operating costs discourage its use. High energy X-ray (HEX), which is the most widely used beam type in radiotherapy, penetrates deeply, has a small divergence, and is affordable. Unfortunately, it is difficult to generate ultrahigh dose rate HEX (HEX-FLASH) mainly because it requires use of ultrahigh beam current (e.g., the minimum requirement of mean current in FLASH irradiation is several mAs for HEXs while only dozens of μAs for electrons are available); hence, it has not been used in in vitro or in vivo FLASH research to the best of our knowledge.

This study aimed to evaluate whether high-energy X-rays (HEXs) of PARTER (platform for advanced radiotherapy research) platform built on CTFEL (Chengdu THz Free Electron Laser facility) can produce ultrahigh dose rate X-rays and trigger a FLASH effect.

Methods and materials

Irradiation devices

HEX-FLASH irradiation was performed using the PARTER platform at the CTFEL [25–26], Chengdu, China, in which the superconducting linac can produce 6–8 MeV electrons with an adjustable mean current of up to 10 mA and an energy spread of less than 0.2% (root mean square measured at a beam energy of 8.2 MeV) (Supplementary 1). For comparison, irradiation with CONV doses was performed using a 6 MV beam from a clinical Elekta Precise linac (Elekta AB, Stockholm, Sweden) in the Mianyang Central Hospital.

Dosimetry

Gafchromic™ EBT3 radiochromic films (Ashland Inc., Covington, Kentucky, USA) were used for absolute dose measurement. Before the FLASH experiment, the EBT3 film was calibrated using a 6 MV beam from a clinical Elekta Precise linac and a farmer ionization chamber FC65-G (IBA Dosimetry GmbH, No. 1463) associated with an IBA DOSE1™ electrometer (Supplementary 2). In the FLASH irradiation, a $CeBr_3$ scintillator was mounted downstream of the mice as a dose monitor (Supplementary 2) At the time of irradiation of each mouse, EBT3 film was inserted between the mice and the PMMA holder (Fig. 1a) to measure the dose delivered to each mouse. Two fast current transformer (FCT) devices, named FCT1 and FCT2, were installed in the accelerator for nondestructive measurement of the pulsed beam current (Supplementary 3). As a general procedure, Monte Carlo computing (MCC) was performed using the Geant4 [27] platform. The bremsstrahlung target, collimator, and the sample were carefully modeled to obtain the dose distribution on the PARTER platform. The accurate parameters of the electron beam were measured by the FCT devices and used as the input to the MCC. The accuracy of the MCC results were validated by EBT3 film measurements.

Animal experiment and ethics statement

Three independent experiments were performed to study the tumor control, damage to the normal lung tissue (whole-thorax irradiation), and intestine (whole-abdomen irradiation) of FLASH and CONV radiotherapies.

For the tumor control experiment, we subcutaneously inoculated EMT6 mouse breast cancer cells into the back skin of six - week-old BAL b/c female mice. The diameter of the tumors had reached approximately 12–15 mm at the time of irradiation. The tumor-bearing mice were divided into three groups: a control group (0 Gy/1F, n = 30), FLASH group (18 Gy/1F, 8 MeV, 1000 Gy/s, n = 15), and CONV group (15 Gy/1F, 6 MeV, 0.1 Gy/s, n = 15). The radiation field was square shaped with the length of sides 1.5 cm to cover the tumor.

For the whole-thorax irradiation experiment, the six-week-old C57BL/6 female mice were divided into three groups: control (0 Gy/1F, n = 18), FLASH group (30 Gy/1F, 8 MeV, 1200 Gy/s, n = 20), and CONV group groups (24 Gy/1F, 6 MeV, 0.1 Gy/s, n = 20). An irradiation field of 2 cm (lateral) × 2 cm (craniocaudal) was used to cover the whole thorax. The upper limit of the irradiation field reached the auricle's lower edge in natural condition.

For the whole-abdomen irradiation experiment, the six-week-old C57BL/6 female mice were divided into three groups: control (0 Gy/1F, n = 18), FLASH group (15 Gy/1F, 8 MeV, 937 Gy/s, n = 20), and CONV group groups (12 Gy/1F, 6 MeV, 0.1 Gy/s, n = 20). An irradiation field of 2 cm (lateral) × 4 cm (craniocaudal) was used to cover the whole abdomen. The upper edge of the irradiation field was defined as the lower part of the thorax (2 cm below the lower edge of the auricle).

Five mice from each group were euthanized at 72 h post-irradiation (pi) for Hematoxylin and eosin (HE) and Masson's trichrome staining of lung and intestine. We used a microscope to observe the normal tissue sections stained with HE at 200 or 400 times magnification. Other mice were observed for 63 days. Mice survivals were checked every day and the tumor sizes were checked every other day. The tumor volume was calculated as V = 0.52 × long diameter × (short diameter) [2].

To eliminate the interferences occurring owing to lethal doses and inconsistencies in the administered total doses in FLASH and CONV radiotherapies, the whole-thorax and whole-abdomen irradiation experiments were repeated, and the total doses delivered with CONV and FLASH irradiation were strictly controlled and verified. We chose six-week-old BAL b/c female mice, as these are reported to have better radiotolerance [28], and strictly verified that an equal dose (30 Gy) was delivered to the whole thorax in a single fraction of FLASH (700 Gy/s, 6 MeV, n = 8), and CONV (0.1 Gy/s, 6 MeV, n = 7) irradiation. The same procedure was performed on their abdomens except that the total dose was set to 12 Gy for the FLASH (700 Gy/s, 6 MeV, n = 8) and CONV groups (0.1 Gy/s, 6 MeV, n = 8); 8 mice were used as the control sample for both thorax and abdomen irradiation. (Experiment details have been summarized in supplementary 4).

All the mice mentioned in this paper were purchased from Sichuan University, Chengdu China. Before the experiments were conducted, approval regarding animal ethics was obtained from the Animal Ethics Committee of Mianyang Hospital (approval number: P2020032). For animal experiments, we followed guidelines of assessment for human end-points in animal experiments published in 2018, in China.

Statistics analyses

We calculated the average tumor volume in the tumor-bearing mice and overall survival of mice irradiated at different dose rates. Statistical analysis was performed using GraphPad Prism v.8.4.0 (GraphPad, La Jolla, CA) software. Single factor analysis of variance (ANOVA) was used to analyze the changes in the mean tumor volumes of tumor-bearing mice in the three groups. Results were expressed as mean values ± standard deviation. Survival curves

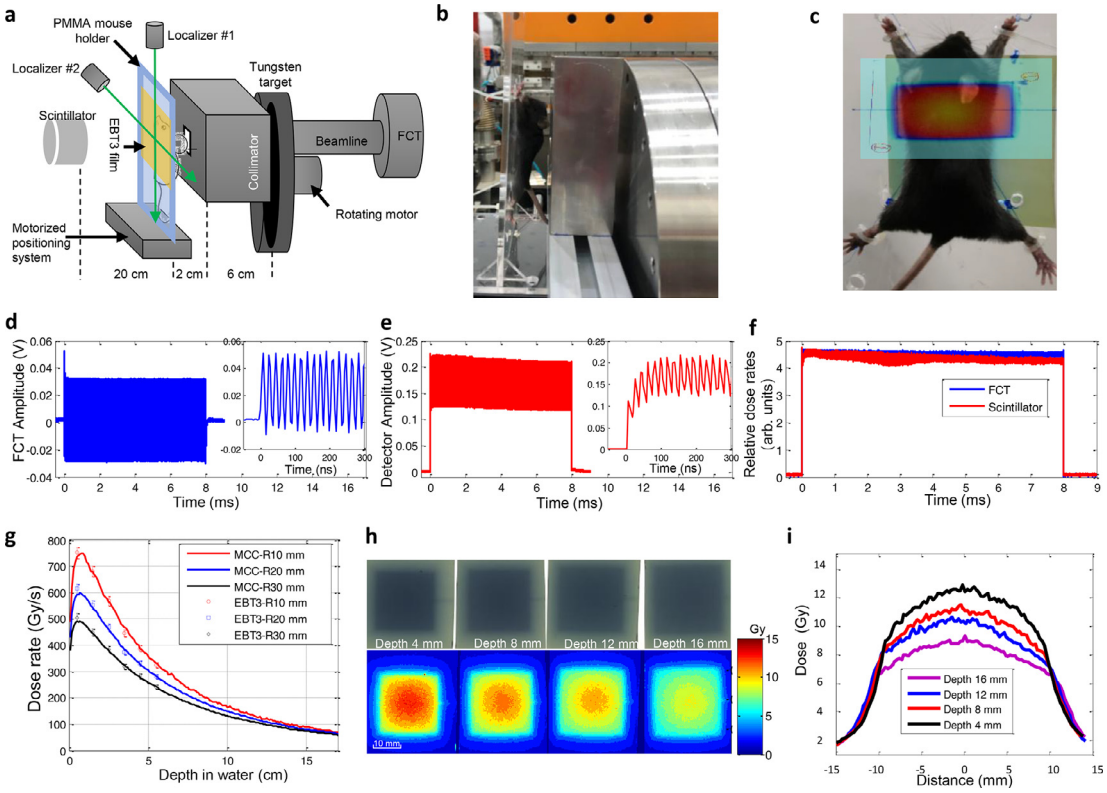

Fig. 1. Parameters and results of the basic HEX-FLASH experiment on PARTER. (a) The schematic diagram of the HEX-FLASH experiment on PARTER. (b) A mouse was fixed on the PMMA holder while being exposed to FLASH irradiation, and (c) a EBT3 film was stuck on the backside of the holder to verify the location of the irradiation field in the mouse and to assist with dose measurement. (d) The current and pulse width of the linac measured using FCTs with a time resolution of nanoseconds, installed on the beamline, and (e, f) the time histories were compared with those obtained using the scintillator. To measure the dose rate and distribution, six EBT3 films were mounted at various depths from 4 mm to 55 mm in the solid water phantom, which is located at the sample position 7 cm behind the rear surface of the target chamber and irradiated using a HEX beam of 7 MeV/3.8 mA. (g) The mean dose rate was given by the total dose measured by film divided by the time of delivery measured by the FCT and Scintillator. The mean dose rates within three different radii (R10, R20, and R30 mm) in the EBT3 films agree with the MCC results based on the beam current given by FCT with a discrepancy of 1% at most of the points and approximately 3% near the surface. Smaller radii show higher mean dose rates because of the center-edge dose attenuation, and the maximum mean dose rate within R10 mm, achieved at 0.5 cm depth, was approximately 750 Gy/s. The dose distribution in the phantom was measured before every biological experiment. (h) Four EBT3 films were mounted at a depth of 4–16 mm of the PMMA phantom behind the collimator window (2 × 2 cm) and were irradiated for 15 ms by a HEX beam of 6 MeV/5.35 mA. (i) 2D dose distribution and profiles in the x-direction in each film. HEX: high-energy X-rays; PARTER: platform for advanced radiotherapy research; PMMA: poly(methyl methacrylate); FCT: fast current transformer; MCC: Monte Carlo computing; R:radius.

were compared using the Kaplan–Meier method with a log-rank test. All statistical tests were conducted at a significance level of 5%, and a two-tailed p-value < 0.05 indicated a statistically significant difference; 95% CIs were also calculated.

Results

The high-energy electron beam produced by the superconducting linac on CTFEL was guided to bombard the rotating tungsten target on PARTER and converted to bremsstrahlung X-rays for FLASH irradiation (Fig. 1a–c). This procedure was essentially the same as that in the CONV radiotherapy machine; thus, the energy spectra of HEX on PARTER were similar to those of the CONV radiotherapy machine; this was confirmed by MCC [29].

The dose rate was a critical parameter that was carefully measured to monitor the implementation of FLASH. The absolute dose measured using medical radiochromic films (EBT3) showed good agreement (discrepancy < 4%) with MCC results, which were based on the electron number given by the FCT device. The time structure, mainly include the length of the macro pulse and period of the micro pulse, was measured using the FCT and $CeBr_3$ scintillator (Fig. 1d, e) and agreed with the preset parameter of the linac. The time histories of the dose rate given by the scintillator monitor and the FCT showed good agreement (<1%), while approximately 5% discrepancy was observed after approximately 1 ms when the beam power was higher than 40 kW (Fig. 1f). This discrepancy might have been induced by beam energy attenuation and has been corrected in the total dose. Both measurements and MCC results showed that in an irradiation field with a diameter of 6 cm and at a depth of over 15 cm in water, the HEX dose rate produced by PARTER was higher than 50 Gy/s (Fig. 1g). The percentage depth dose (PDD) in the sample was adjusted by changing the beam current (1–10 mA) and energy (6–8 MV) of the superconducting linac. In our experiments, the dose rate of FLASH irradiation in mice was 700–1200 Gy/s. As the depth increased, the dose rates dropped rapidly, but the dose uniformity in the irradiation field was improved. When both the collimator window and target area were set as 2 × 2 cm, the dose uniformity ratios (ratio of the maximum dose divided by the minimum dose) were 1.43 and 1.25 at depths of 4 and 16 mm, respectively (Fig. 1h, i). The percent depth dose and dose profiles of the CONV beam are shown in Fig. s1. MCC showed that approximately 9% of the dose deposited at the surface layer (0–2 cm) was produced by leaked high-energy electrons when the beam energy was set to 8 MeV, and the dose from leaked electrons was less than 1% if the depth was over 2 cm or the beam energy was set to 6 MeV. The recommended beam energy for HEX-FLASH in our PARTER platform is 6 MV corresponding to a maximum dose rate of approximately 800 Gy/s in mice. Dose calibration was performed before every biological experiment to verify the status of PARTER and reconfirm the corre-

lation coefficients among the dose rate, beam current, and scintillator current. Correlation coefficients generally varied by less than 3% between each calibration.

For tumor bearing BAL b/c mice, observations at 63 days pi revealed that the growth rates of tumors in the FLASH or CONV groups were slower than those observed in the control group. The slowest increase in tumor volume was observed in the FLASH group, and the difference in tumor volume among the three groups increased with time. The average tumor volume in the control group was 40565.3 ± 8675.8 mm^3 on the 40th day pi, whereas the maximum volumes recorded in the CONV and FLASH groups were approximately 30,000 and 15,000 mm^3 during the entire observation period (Fig. 2a). The difference between the CONV and FLASH groups was statistically significant ($p = 0.0002$ in one-way ANOVA). Significant differences in volumes among the three groups were also validated with ANOVA ($F = 25.14$, $p < 0.0001$). Significant differences ($p < 0.005$) were also observed among the survival curves of the three groups of mice (Fig. 2b); the median survival times were similar in the FLASH (55 days) and CONV (59.5 days) groups, while the control group had a lower (35.5 days) median survival time. We speculated that the possible reason for death was metastasis in the lungs or other parts of the mice.

For healthy C57BL/6 mice exposed to whole-thorax irradiation, Masson special staining of the lung sections showed that alveolar structures were similar between the FLASH and control groups, whereas more disintegrated alveolar structures appeared in the lung sections of the CONV group. Collagenous fiber staining (blue-staining area) around the alveoli was more obvious in the FLASH and CONV group than in the control group. However, under the microscope, the blue-staining area of the FLASH group is light and uniform; otherwise, the blue-staining area of the CONV group seems to be more disorderly (Fig. 2c), suggesting that the degree of alveolar fibrosis is more serious. The retained mice were fed for more than two months, and their survival probability was monitored. In thorax-irradiated mice (Fig. 2d), the survival rate was 100% in the control group, 90% in the FLASH group, and 50% in the CONV group at the end of the observation. The median survival time was not reached in the FLASH group because of the 90% survival rate, although it was 38 days in the CONV group. There was a statistically significant difference ($P = 0.038$) in survival among the three groups. The hazard ratio (HR) was 0.19, 95% confidence intervals (CIs) were 0.035–1.010, and p was 0.0486 between the FLASH and CONV groups; therefore, the risk of death decreased by 81% in the FLASH group compared with that in the CONV group.

For healthy C57BL/6 mice exposed to whole-abdominal irradiation, the small intestines' basic structure still existed; however, the blue-staining areas were found different in all three groups (Fig. 2e). The blue-staining area of the control group was close to

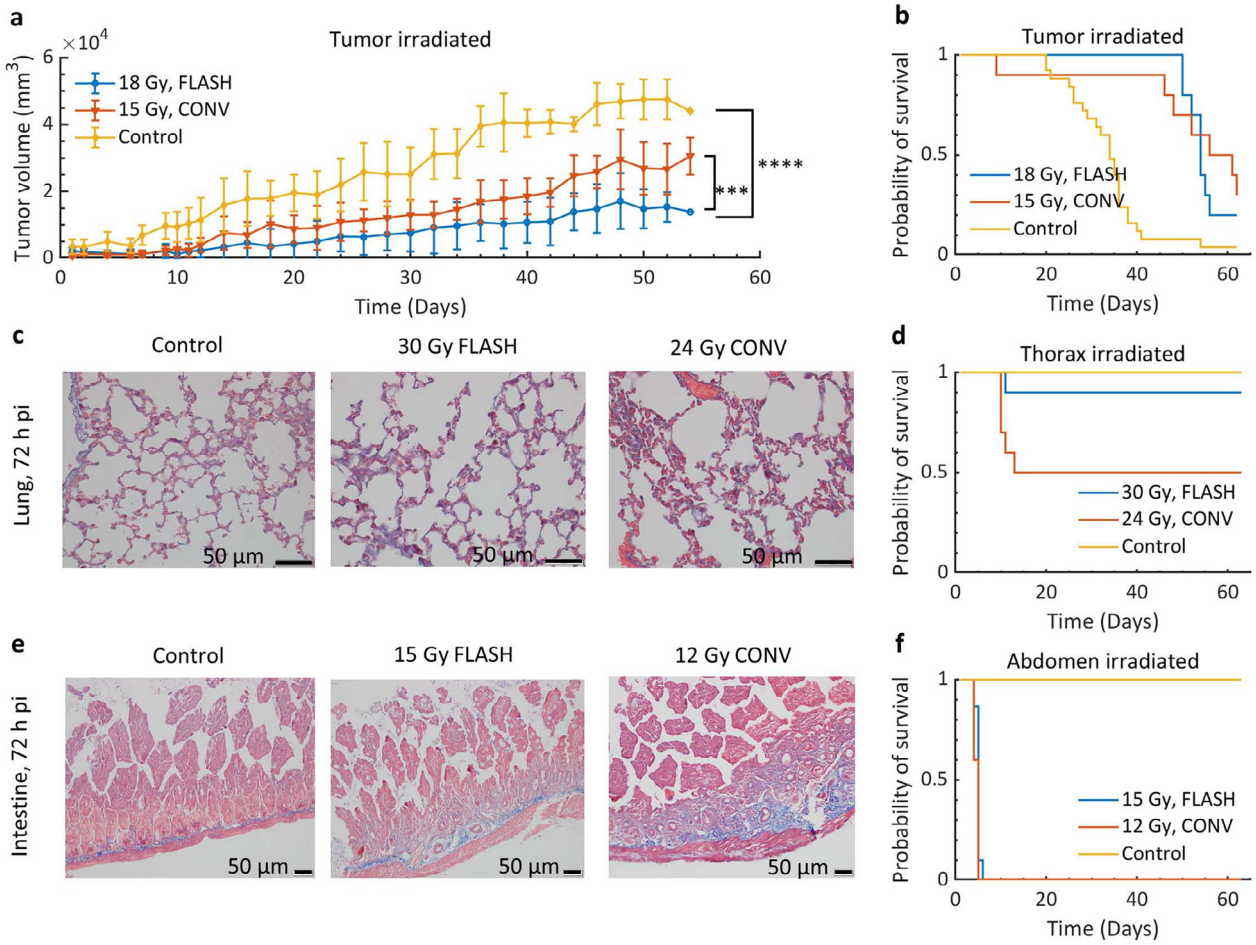

Fig. 2. (a) Evolution of EMT6 tumor homografts in BAL b/c mice. (b) Survival curves of tumor-bearing BAL b/c mice in the control ($n = 30$), FLASH (18 Gy/1F, 8 MeV, 1000 Gy/s, $n = 15$) and conventional (CONV) (15 Gy/1F, 6 MeV, 0.1 Gy/s, $n = 15$) groups respectively. (c) Masson special staining of the lung tissue of healthy C57BL/6 mice under microscope. (d) Survival curves of healthy C57BL/6 mice of in the control ($n = 18$), FLASH (30 Gy/1F, 8 MeV, 1200 Gy/s, $n = 20$) and CONV (24 Gy/1F, 6 MeV, 0.1 Gy/s, $n = 20$) groups that received thorax irradiation (e) Masson special staining of the small intestine tissue of healthy C57BL/6 mice under microscope. (f) Survival curves of healthy C57BL/6 mice in the control ($n = 18$) FLASH (15 Gy/1F, 8 MeV, 937 Gy/s, $n = 20$) and CONV (12 Gy/1F, 6 MeV, 0.1 Gy/s, $n = 20$) group that received abdominal irradiation. pi: post-irradiation. p-values were derived with one-way repeated ANOVA: $^{***}p < 0.001$, $^{****}p < 0.0001$.

muscularis propria and was very uniform and thin, while the blue-staining area of other two groups was uneven and thick, especially in the CONV group. The blue-staining area revealed that the inflammatory reaction after radiotherapy led to regeneration of collagen fibers. The staining degree of FLASH group was between that of control group and the CONV group. In the CONV group, collagenous fibers staining was not only in the vicinity of the muscularis propria, but it also extended to the periphery of the glandular duct (Fig. 2e). In abdomen-irradiated mice (Fig. 2f), the survival rate was 100% in the control group at 63 days pi, but all mice in the FLASH and CONV groups died from radiation-induced enteritis at 4–5 days pi with no statistically significant difference.

In the equal dose experiment, the median survival times of thorax-irradiated mice in the FLASH (120 days) and CONV groups (86 days) (Fig. 3a) were statistically different (HR 0.187; 95% CI 0.044–0.803; $p < 0.0001$), mice of two groups died from radiation-induced pneumonia. With abdominal irradiation, the FLASH group displayed obviously better survival curves than the CONV group in which all mice lived for less than 10 days pi. (Fig. 3b). In the FLASH group, 62.5% of the mice were still alive when we stopped observation; therefore, we could not obtain a value for the median survival time. The survival time of mice in the FLASH group was undoubtedly higher than that in the CONV group (7 days); the difference in survival between the two groups was marginally significant (HR 0.369; 95% CI 0.113–1.202; $p = 0.0735$). Despite this, the survival trend of mice treated with HEX-FLASH radiotherapy was better.

Discussion

A critically important problem of this study was the precision of the dosimetric system; the system consisted of an EBT3 film, FCT beam monitor, and a scintillator dosimeter. The dose uncertainty given by this system was ±5%, higher than that in CONV (generally ±2%); the range of deviation was acceptable for a prototype [30]. The real-time dose rate in the sample during irradiation, computed according to the beam current given by FCT, differed from that estimated by the scintillator, especially in the early macro-pulse with high beam current. The discrepancy was because of energy attenuation in the linac. In addition, although only EBT3 film was used in this study, a new EBT-XD film was scheduled to extend its dose range to over 40 Gy. Compared with CONV radiotherapy, the ultrashort irradiation time is a significant advantage of FLASH, but it is also a big challenge for the real-time adjustment of the current and width of the macro pulse of the linac. In the present HEX-FLASH study, the energy/current of the linac and width of the macropulse are preset based on calibration and computing data, but the inevitable power fluctuation of the linac during real-time irradiation leads to an actual dose that differs from the theoretical value (usually ±5%). Although we had considered this fluctuation in the dose design and that a large sample number can partially counteract this effect in animal experiments, the interaction between the dosimetric system and linac is an important consideration for more precise experimentation and future clinical application. A variety of dose rates are used throughout this work, because it is difficult to control the dose rate at each experiment very exactly, we expect all cases above 40 Gy/s to have the same FLASH effect.

In experiments determining the anti-tumor effects of HEX-FLASH, we observed significant differences in tumor growth delay among the three groups (control, CONV, and FLASH groups), consistent with the results reported by Favaudon et al [5]. HEX-FLASH radiotherapy showed a surprisingly excellent tumor control efficiency, the tumor volume of three groups was statistically different, although the subcutaneous tumor volume was a bit larger than ideal at the time of irradiation, owing to the long waiting time for the setting up of PARTER and getting permission for experiments (there was a one week delay due to the 2019-nCoV outbreak in China), and the volume of tumor had therefore reached 150 mm^3 at the time of irradiation. However, this superior tumor control effect shown by HEX-FLASH radiotherapy may be because of the 20% higher dose used in HEX-FLASH radiotherapy than in CONV radiotherapy. In fact, it was previously reported that the same dose FLASH and CONV radiotherapy have equivalent tumor control efficiency [31,32]. In addition, guideline of assessment for human endpoints in animal experiments requires that tumor-bearing mice be killed when the tumor volume exceeds 3000 mm^3 to alleviate the pain of experimental animals. However, during the preparation period of the experiment, the 2019-nCoV outbroke in China. Considering the novelty and difficulty of this study, we put forward to the Ethics Committee that we would like to observe the survival of tumor-bearing mice at the same time. After obtaining the approval of the Ethics Committee of our hospital, we continued to feed the mice to collect more data on survival and tumor volume.

The tumor volume was plotted only until day 54 pi because only 1, 3, and 6 mice survived in the control, FLASH, and CONV group, respectively; subsequent data were considered statistically

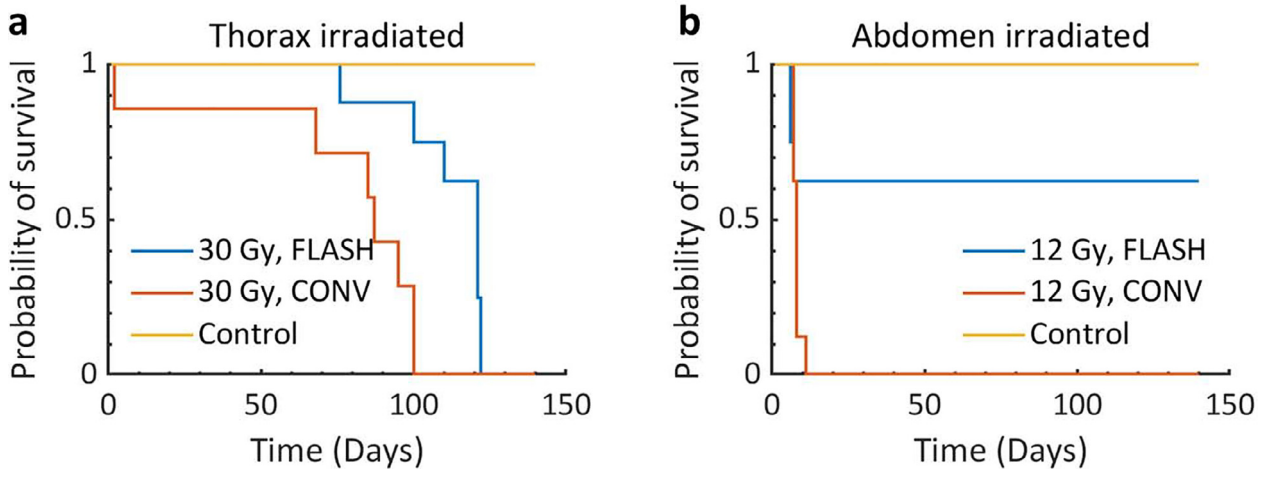

Fig. 3. (a) Survival curves of healthy BAL b/c mice of the control ($n = 8$), FLASH (30 Gy/1F, 700 Gy/s, 6 MeV, $n = 8$), and CONV (30 Gy/1F, 0.1 Gy/s, 6 MeV, $n = 7$) groups that received thorax irradiation. (b) Survival curves of healthy BAL b/c mice of the control ($n = 8$), FLASH (12 Gy/1F, 700 Gy/s, 6 MeV, $n = 8$), and CONV (12 Gy/1F, 0.1 Gy/s, 6 MeV, $n = 8$) groups that received abdominal irradiation.

uncertain. However, the survival data were not affected. In the whole-thorax irradiation experiments, although the total dose was 20% higher in the FLASH group than in the CONV group, the FLASH group displayed protective effects on the lung tissue. The survival curve for CONV exhibits an unusual shape, reaching 50% survival very quickly, and then plateauing, the similar phenomenon has appeared in the previous literature [33–35], but the exact reasons of this phenomenon need further research. This result is a powerful evidence that HEX-FLASH radiotherapy has protective effects on normal tissues. However, in the whole-abdomen irradiation experiments, HEX-FLASH radiotherapy showed no protective effects. A possible explanation for this result is that different tissues have different tolerance rates to radiation; for example, the median lethal dose (LD50) of the small intestine is significantly lower than that of the lung in CONV radiotherapy [29,36,37]. Owing to poor radio tolerance of the small intestine, the dose delivered to the abdomen in the CONV group was already its lethal dose. When a 25% higher dose was delivered in the FLASH group, the mice died immediately. Thus, the protective effects of FLASH were masked. In the equal dose experiment, when the same dose of 12 Gy was delivered to the abdomen with FLASH or CONV, a better survival trend was observed in the FLASH group than the CONV group. This result is consistent with other studies that reported the radio-protective effect of FLASH irradiation on the intestine [31,32,38].

The main limitation of this study was that the total dose was inconsistent in CONV and FLASH groups, and it was indeed difficult to conclude whether differences are due to a FLASH effect or from the increased dose. Since the FLASH effect is significant in the protection of normal tissue. Moreover, this is the first time we have run an experiment on PARTER, and we have some concerns about the stability of the machine. Considering the instability of the machine, we prefer to make the total dose of the FLASH group higher, so that our experimental results are also illustrative, if the total dose of the flash group is lower, then our experimental results are meaningless. Of course, we admit that this is a limiting factor of our experiment. In future experiments, we will aim to adjust the study design and answer this question scientifically.

In summary, this study was conducted in two parts. Firstly, the generation of HEX-FLASH by the PARTER system and its physical properties were confirmed. Secondly, the positive FLASH effects triggered by HEX were observed. The current study provides a basis for future scientific research and clinical application of HEX in FLASH radiotherapy.

Acknowledgments

This work was financially supported by the National Natural Science Foundation of China (NSFC grant nos. 11975218, 11905210, 11805192, 12005211, and 11605190) and Innovation Foundation of CAEP (grant nos. CX2019036 and CX2019037).

Conflict of interest

The authors have no known conflicts of interest to declare.

Appendix A. Supplementary data

Supplementary data to this article can be found online at https://doi.org/10.1016/j.radonc.2021.11.004.

References

[1] Bray F, Ferlay J, Soerjomataram I, Siegel RL, Torre LA, Jemal A. Global cancer statistics 2018: Globocan estimates of incidence and mortality worldwide for 36 cancers in 185 countries. CA 2018;68:394–424. https://doi.org/10.3322/caac.21492.
[2] Steel Gordon G. Basic clinical radiobiology. London: Edward Arnold Publication; 1993.
[3] Baumann M, Krause M, Overgaard J, Debus J, Bentzen SM, Daartz J, et al. Radiation oncology in the era of precision medicine. Nat Rev Cancer 2016;16:234–49. https://doi.org/10.1038/nrc.2016.18.
[4] Montay-Gruel P, Acharya MM, Petersson K, Alikhani L, Yakkala C, Allen BD, et al. Long-term neurocognitive benefits of flash radiotherapy driven by reduced reactive oxygen species. Proc Natl Acad Sci 2019;116:10943–51. https://doi.org/10.1073/pnas.1901777116.
[5] Favaudon V, Caplier L, Monceau V, Pouzoulet F, Sayarath M, Fouillade C, et al. Ultrahigh dose-rate FLASH irradiation increases the differential response between normal and tumor tissue in mice. Sci Transl Medicine 2014;6:245ra93. https://doi.org/10.1126/scitranslmed.3008973.
[6] Montay-Gruel P, Acharya MM, Gonçalves Jorge P, Petit B, Petridis IG, Fuchs P, et al. Hypo-fractionated flash-rt as an effective treatment against glioblastoma that reduces neurocognitive side effects in mice. Clin Cancer Res 2021;27:775–84. https://doi.org/10.1158/1078-0432.CCR-20-0894.
[7] Venkatesulu BP, Sharma A, Pollard-Larkin JM, Sadagopan R, Symons J, Neri S, et al. Ultra high dose rate (35 Gy/sec) radiation does not spare the normal tissue in cardiac and splenic models of lymphopenia and gastrointestinal syndrome. Sci Reports 2019;9:17180. https://doi.org/10.1038/s41598-019-53562-y.
[8] Chabi S, To THV, Leavitt R, Poglio S, Jorge PG, Jaccard M, et al. Ultra-high dose rate FLASH and conventional dose rate irradiation differentially affect human acute lymphoblastic leukemia and normal hematopoiesis. Int J Radiat Oncol 2021;109:819–29. https://doi.org/10.1016/j.ijrobp.2020.10.012.
[9] Soto LA, Casey KM, Wang J, Blaney A, Manjappa R, Breitkreutz D, et al. Flash irradiation results in reduced severe skin toxicity compared to conventional-dose-rate irradiation. Radiat Res 2020;194. https://doi.org/10.1667/RADE-20-00090.
[10] Montay-Gruel P, Bouchet A, Jaccard M, Patin D, Serduc R, Aim W, et al. X-rays can trigger the flash effect: ultra-high dose-rate synchrotron light source prevents normal brain injury after whole brain irradiation in mice. Radiother Oncol 2018;129:582–8. https://doi.org/10.1016/j.radonc.2018.08.016.
[11] Loo BW, Schuler E, Lartey FM, Rafat M, King GJ, Trovati S, et al. (p003) Delivery of ultra-rapid flash radiation therapy and demonstration of normal tissue sparing after abdominal irradiation of mice. Int J Radiat Oncol 2017;98. https://doi.org/10.1016/j.ijrobp.2017.02.101.
[12] Montay-Gruel P, Petersson K, Jaccard M, Boivin G, Germond J-F, Petit B, et al. Irradiation in a flash: unique sparing of memory in mice after whole brain irradiation with dose rates above 100 Gy/s. Radiother Oncol 2017;124:365–9. https://doi.org/10.1016/j.radonc.2017.05.003.
[13] Vozenin MC, De Fornel P, Petersson K, Favaudon V, Jaccard M, Germond JF, et al. The advantage of FLASH radiotherapy confirmed in mini-pig and cat-cancer patients. Clin Cancer Res 2019;25:35–42. https://doi.org/10.1158/1078-0432.CCR-17-3375.
[14] Levy K, Rafat M, Casey K, Rankin E. Total abdominal ultra-rapid flash irradiation decreases gastrointestinal toxicity compared to conventional radiation. Gynecol Oncol 2019;154:75. https://doi.org/10.1016/j.ygyno.2019.04.177.
[15] Bourhis J, Sozzi WJ, Jorge PG, Gaide O, Bailat C, Duclos F, et al. Treatment of a first patient with FLASH-radiotherapy. Radiother Oncol 2019;139:18–22. https://doi.org/10.1016/j.radonc.2019.06.019.
[16] Medical, V. Feasibility study of FLASH radiotherapy for the treatment of symptomatic bone metastases (fast-01). [EB/OL]. 2020; https://clinicaltrials.gov/ct2/show/study/NCT04592887.
[17] Vozenin M-C, Hendry J, Limoli C. Biological benefits of ultra-high dose rate flash radiotherapy: sleeping beauty awoken. Clin Oncol 2019;31:407–15. https://doi.org/10.1016/j.clon.2019.04.001.
[18] Fouillade C, Curras-Alonso S, Giuranno L, Quelennec E, Heinrich S, Bonnet-Boissinot S, et al. Flash irradiation spares lung progenitor cells and limits the incidence of radio-induced senescence. Clin Cancer Res 2020;26:1497–506. https://doi.org/10.1158/1078-0432.CCR-19-1440.
[19] Simmons DA, Lartey FM, Schüler E, Rafat M, King G, Kim A, et al. Reduced cognitive deficits after flash irradiation of whole mouse brain are associated with less hippocampal dendritic spine loss and neuroinflammation. Radiother Oncol 2020;139:4–10. https://doi.org/10.1016/j.radonc.2019.06.006.
[20] Bourhis J, Montay-Gruel P, Gonçalves Jorge P, Bailat C, Petit B, Ollivier J, et al. Clinical translation of flash radiotherapy: Why and how? Radiother Oncol 2020;139:11–7. https://doi.org/10.1016/j.radonc.2019.04.008.
[21] Smyth LML, Donoghue JF, Ventura JA, Livingstone J, Bailey T, Day LRJ, et al. Comparative toxicity of synchrotron and conventional radiation therapy based on total and partial body irradiation in a murine model. Sci Rep 2018;8. https://doi.org/10.1038/s41598-018-30543-1.
[22] Zlobinskaya O, Siebenwirth C, Greubel C, Hable V, Hertenberger R, Humble N, et al. The effects of ultra-high dose rate proton irradiation on growth delay in the treatment of human tumor xenografts in nude mice. Radiat Res 2014;181:177–83. https://doi.org/10.1667/RR13464.1.
[23] Beyreuther E, Brand M, Hans S, Hideghéty K, Karsch L, Leßmann E, et al. Feasibility of proton flash effect tested by zebrafish embryo irradiation. Radiother Oncol 2019;139:46–50. https://doi.org/10.1016/j.radonc.2019.06.024.
[24] Rama N, Saha T, Shukla S, Goda C, Milewski D, Mascia AE, et al. Improved tumor control through t-cell infiltration modulated by ultra-high dose rate

proton flash using a clinical pencil beam scanning proton system. Int J Radiat Oncol 2019;105:S164–5. https://doi.org/10.1016/j.ijrobp. 2019.06.187.
[25] Ming, Li, Xingfan Yang, Zhou Xu, Xiaojian Shu, Xiangyang Lu, Wenhui Huang et al. First lasing of CAEP THz free electron laser. High Power Laser Part. Beams. 2017; 29, 100101, 10.11884/HPLPB201729.170363.
[26] Wu D, Li M, Yang X, Wang H, Luo X, Shen X, et al. First lasing of the CAEP THz FEL facility driven by a superconducting accelerator. J Physics: Conf Ser 2018;1067:. https://doi.org/10.1088/1742-6596/1067/3/032010032010.
[27] Agostinelliae S, Allisonas J, Amako K, Apostolakis J, Araujo H, Arce P, et al. Geant4—a simulation toolkit. Nucl Instruments Methods Phys Res Sect A: Accel Spectrometers, Detect Assoc Equip 2003;506:250–303. https://doi.org/10.1016/S0168-9002(03)01368-8.
[28] Mukherjee S, Sainis K, Deobagkar DD. F 1 hybrids of balb/c and c57bl/6 mouse strains respond differently to low-dose ionizing radiation exposure. J Genetics 2014;93:667–82.
[29] Feng, G. Lulu, Cao, Yiwei Yang, Xiaobo Du, Tangzhi Dai, Dai Wu. Design and calculation of Flash-RT based on PARTER. Chin. J. Med. Phys. 2020;37, 1081–1087, 10.3969/j.issn.1005-202X.2020.09.001.
[30] Shalek RJ. Determination of absorbed dose in a patient irradiated by beams of x or gamma rays in radiotherapy procedures. Med Phys 1997;4:461. https://doi.org/10.1118/1.594356.
[31] Diffenderfer ES, Verginadis II, Kim MM, et al. Design, implementation, and in vivo validation of a novel proton FLASH radiation therapy system. Int J Radiat Oncol Biol Phys 2020;106:440–8. https://doi.org/10.1016/j.ijrobp.2019.10.049.
[32] Levy K, Natarajan S, Wang J, Chow S, Eggold JT, Loo PE, et al. Abdominal FLASH irradiation reduces radiation-induced gastrointestinal toxicity for the treatment of ovarian cancer in mice. Sci Rep 2020;10. https://doi.org/10.1038/s41598-020-78017-7.
[33] Li Y, Dong J, Xiao H, Zhang S, Wang B, Cui M, et al. Gut commensal derived-valeric acid protects against radiation injuries. Gut Microbes 2020;11:789–806. https://doi.org/10.1080/19490976.2019.1709387.
[34] Bensemmane L, Squiban C, Demarquay C, Mathieu N, Benderitter M, Le Guen B, et al. The stromal vascular fraction mitigates radiation-induced gastrointestinal syndrome in mice. Stem Cell Res Ther 2021;12. https://doi.org/10.1186/s13287-021-02373-y.
[35] Lee CL, Daniel AR, Holbrook M, Brownstein J, Silva Campos LD, Hasapis S, et al. Sensitization of vascular endothelial cells to ionizing radiation promotes the development of delayed intestinal injury in mice. Radiat Res 2019;192:258. https://doi.org/10.1667/RR15371.1.
[36] Booth C, Tudor G, Tudor J, Katz B, MacVittie T. Acute gastrointestinal syndrome in high-dose irradiated mice. Heal Phys 2012;103:383–99. https://doi.org/10.1097/HP.0b013e318266ee13.
[37] Hanson WR, Fry RJM, Sallese AR, Frischer H, Ahmad T, Ainsworth EJ. Comparison of intestine and bone marrow radiosensitivity of the balb/c and the c57bl/6 mouse strains and their b6cf1 offspring. Radiat Res; (United States) 1987;110:340. https://doi.org/10.2307/3577002.
[38] Ruan JL, Lee C, Wouters S, Tullis IDC, Verslegers M, Mysara M, et al. Irradiation at ultra-high (FLASH) dose rates reduces acute normal tissue toxicity in the mouse gastrointestinal system. Int J Radiat Oncol Biol Phys 2021. https://doi.org/10.1016/j.ijrobp.2021.08.004.